Supplementary information

Targeting chaperone-mediated autophagy inhibits properties of glioblastoma stem cells and restores anti-tumor immunity

Yonghua Li, Min Sheng, Weijie Li, Simin Liu, Botao Wang, Bing Liu, Mei Luo, Xiao Zhou, Qiaoxi Xia, Shihong Hong, Ziyuan Zheng, Shi-Yuan Cheng, Xiaobing Jiang, Junjun Li, and Tianzhi Huang

Table of contents

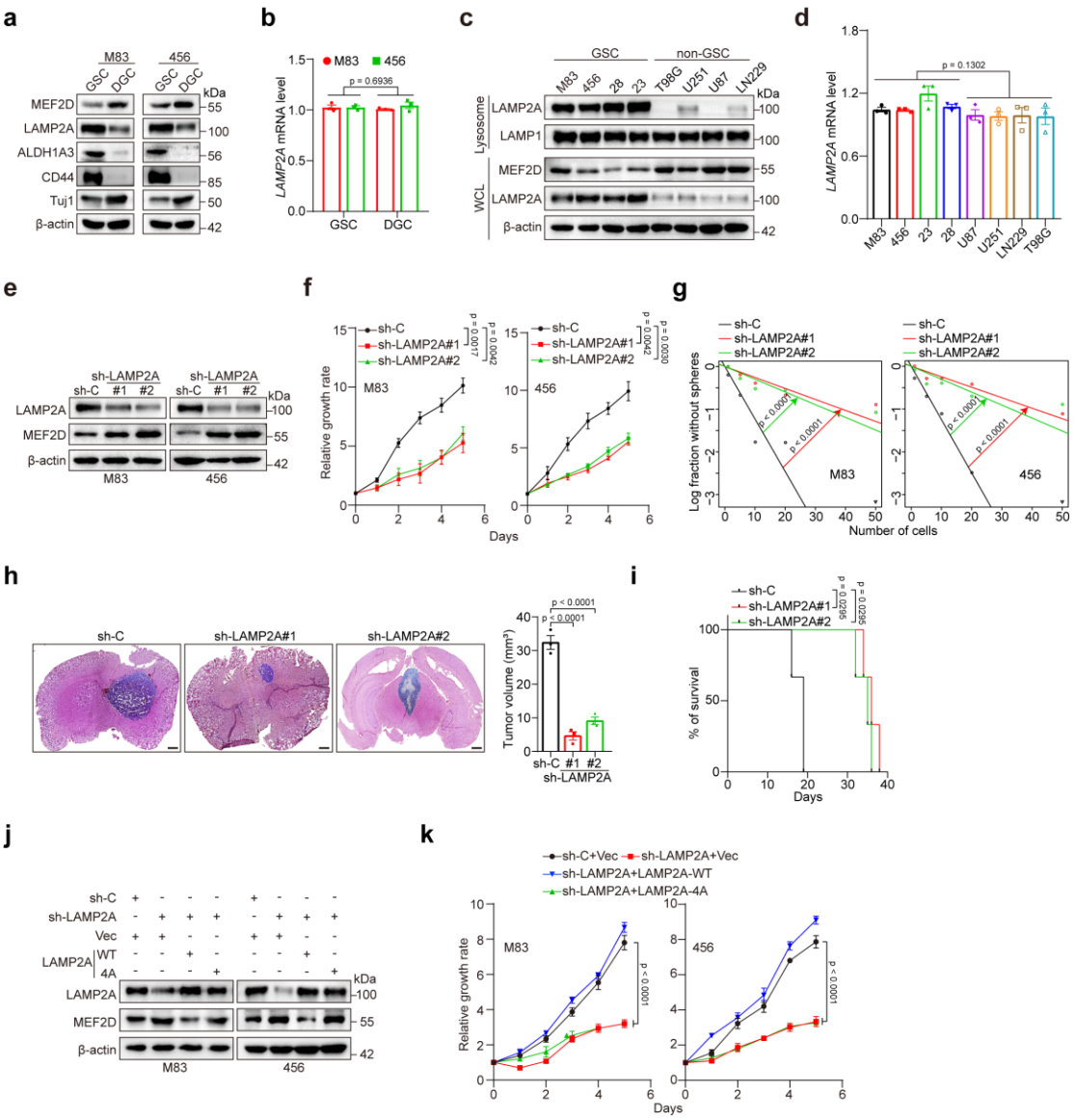

Supplementary Figure 1: Increased LAMP2A expression in GSCs is correlated with higher CMA activity and greater tumorigenic potential. a Immunoblot (IB) for indicated proteins in GSC M83 and 456 cells and their corresponding DGCs. **b**, **d** Quantitative real-time PCR (qPCR) assessment of *LAMP2A* mRNA level in GSCs and DGCs (**b**) or in GSCs and non-GSCs (**d**). n = 3 independent experiments. **c** IB analyses for LAMP2A and MEF2D, CMA targets, in whole-cell lysates (WCL) and lysosomal fractions of GSCs and non-GSCs. β-actin and LAMP1 were used as loading controls for WCL and lysosomal samples, respectively. **e** IB analyses for LAMP2A and MEF2D in GSC M83 and 456 cells expressing sh-C or sh-LAMP2A. **f**, **g** Cell proliferation (**f**) and Sphere-forming frequency (**g**) of GSC M83 and 456 cells expressing sh-C or sh-LAMP2A. n = 3 independent experiments in (**f**). **h**

Representative H&E images of mouse brain sections (left) and quantification of tumor volume (right) from athymic (BALB/c Nude) mice intracranially implanted with GSC M83 cells with indicated modifications. n = 3 mice per group. Scale bar, 1.0 mm. **i** Kaplan-Meier survival curves for athymic (BALB/c Nude) mice intracranially transplanted with GSC M83 cells with indicated modifications. n = 3 mice per group. **j** IB analyses for LAMP2A and MEF2D in GSC M83 and 456 cells with indicated modifications. **k** Cell proliferation of GSC M83 and 456 cells with indicated modifications. LAMP2A-4A, functional deficiency mutants of LAMP2A. Data are presented as the means ± S.E.M. All the experiments showed consistent results in at least three independent biological replicates. Statistical significance was assessed using one-way ANOVA with Tukey's multiple comparisons test (**b**, **d**), one-way ANOVA with Dunnett's multiple comparisons test (**f**, **h**, **k**), two-sided likelihood ratio test (**g**) or log-rank test (**i**). ns, not significant. Source data are provided as a Source Data file.

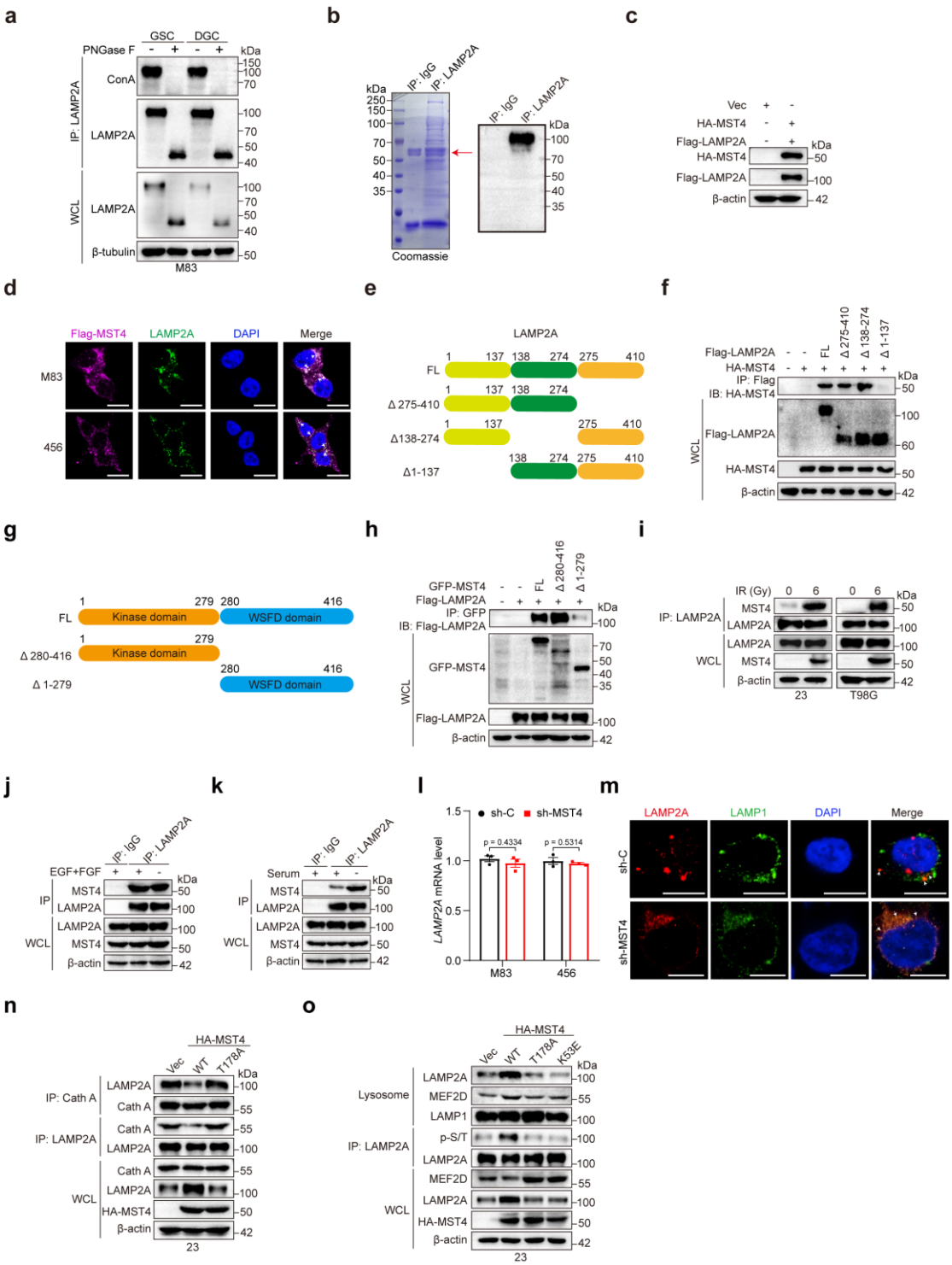

Supplementary Figure 2: MST4 associates with LAMP2A and enhances its stability. a IP-IB analyses for LAMP2A and Concanavalin A (ConA) in GSC and DGC M83 cells with or without PNGase F treatment. **b** Immunoprecipitation assays utilizing an anti-LAMP2A antibody or a control IgG were performed, followed by SDS-PAGE analyses (left) and IB detection with an anti-LAMP2A antibody and veriBlot for IP Detection Reagent (HRP) (right). **c** IB analyses for HA-tag and Flag-tag in GSC M83 cells transfected with HA-MST4 and Flag-LAMP2A. **d** Immunofluorescent (IF) staining analyses of GSC M83 and 456 cells overexpressing

Flag-MST4 using anti-LAMP2A and anti-Flag antibodies. Flag-MST4 (magenta), LAMP2A (green). Nuclei were stained with DAPI (blue). Scale bar, 15 μm. **e**, **g** Schematic representation of the domain architecture deletions for LAMP2A (**e**) and MST4 (**g**). **f**, **h** IP-IB analyses for indicated proteins in HEK293T cells for mapping of specific domains responsible for MST4-LAMP2A interaction. **i** IP-IB analyses for the indicated proteins of GSC 23 cells and T98G cells treated with IR (0 or 6 Gy). **j**, **k** IP-IB analyses for indicated proteins in GSC 23 cells under conditions with or without EGF/FGF deprivation (**j**), and in HEK293T cells with or without serum starvation (**k**). **l** qPCR assessment of *LAMP2A* mRNA level in GSC M83 and 456 cells expressing sh-C or sh-MST4. Data are presented as the means ± S.E.M. n = 3 independent experiments. Statistical significance was assessed using two-tailed Student's t-test. ns, not significant. **m** IF staining analyses of GSC M83 cells expressing sh-C and sh-MST4 using anti-LAMP2A and anti-LAMP1 antibodies. LAMP2A (red), LAMP1 (green), DAPI (blue). Scale bar, 10 μm. **n** IP-IB for indicated proteins in GSC 23 cells with indicated modifications. **o** IP-IB for indicated proteins in WCL and lysosomal fractions of GSC 23 cells with indicated modifications. All the experiments showed consistent results in at least three independent biological replicates. Source data are provided as a Source Data file.

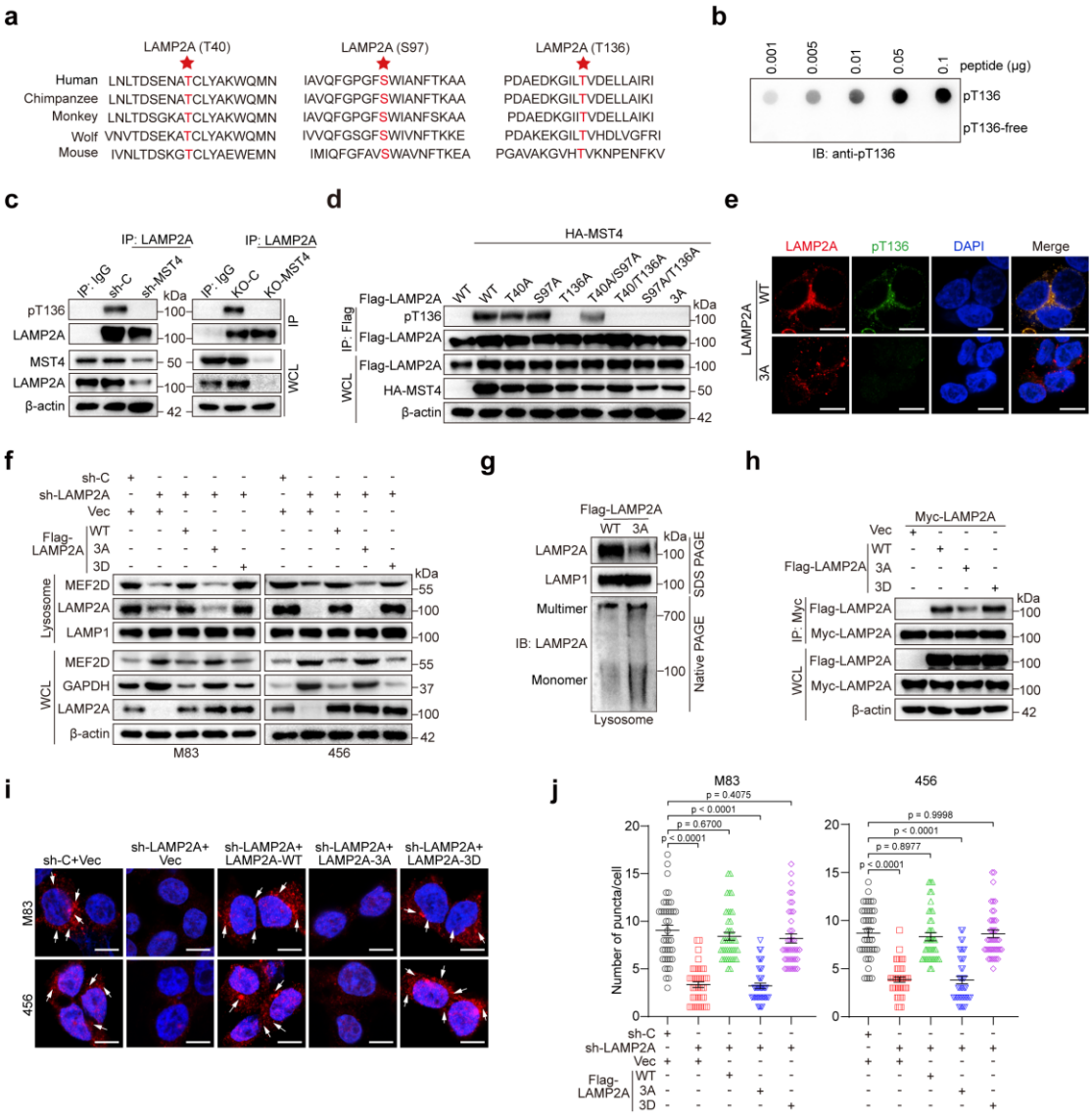

Supplementary Figure 3: MST4-mediated phosphorylation of LAMP2A boosts CMA activity. a Amino acid sequences around Threonine 40 (T40), Serine 97 (S97), Threonine 136 (T136) residues in LAMP2A across different species. Asterisk at the top indicates residue that is conserved across species. **b** Dot blot assay utilizing an antibody specific to the phosphorylated site (pT136) of LAMP2A. **c** IP-IB for indicated proteins in GSC M83 cells with indicated modifications. **d** IP-IB assessments were conducted for Flag-LAMP2A, HA-MST4, and LAMP2A pT136 in HEK293T cells, both under conditions of MST4 and LAMP2A-WT or -Mut overexpression and in their absence. **e** IF staining analyses of GSC M83 cells overexpressing either LAMP2A WT or the 3A mutant, using anti-LAMP2A and anti-LAMP2A pT136 antibodies. LAMP2A (red), LMAP2A pT136 (green), DAPI (blue). Scale bar, 10 μm. **f** IB for indicated proteins in WCL and lysosomal fractions from GSC M83 and 456 cells with indicated modifications. **g** Purified lysosomes from indicated GSC M83 cells were analyzed using SDS-PAGE and native PAGE, and subjected to IB detection for LAMP2A. **h** IP-IB for indicated proteins in GSC M83 cells with

indicated modifications. **i**, **j** Representative images (**i**) and quantification (**j**) of CMA activity detection by KFERQ puncta numbers in GSC M83 and 456 cells with indicated modifications. Data are presented as the means ± S.E.M. Statistical significance was assessed using one-way ANOVA with Dunnett's multiple comparisons test. n = 40 randomly selected cells. Scale bar, 10 μm. All the experiments showed consistent results in at least three independent biological replicates. Source data are provided as a Source Data file.

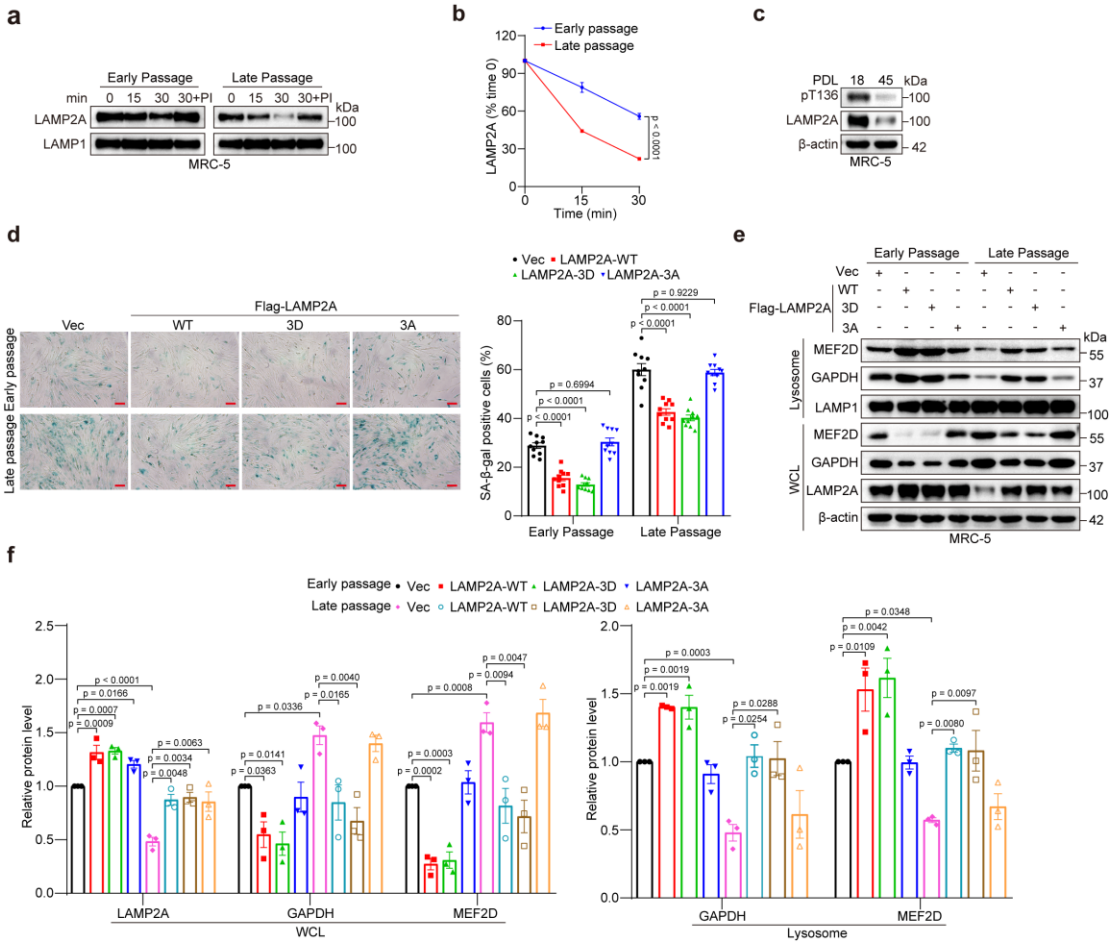

Supplementary Figure 4: Phosphorylation of LAMP2A rescues CMA deficiency in aging cell models. a, **b** Evaluation of LAMP2A stability in lysosomal extracts from indicated GSCs and DGCs. Densitometric quantification of LAMP2A protein level is shown in (**b**). n = 3 independent experiments. **c** IB analyses for indicated proteins in MRC-5 cells of early (P18) and late (P45) passages. PDL, population doubling level. **d** Representative images of senescence-associated beta-galactosidase (SA-β-gal) staining of MRC-5 cells at early (P18) and late (P45) passage with or without overexpressing Flag-LAMP2A-WT/3D/3A. Quantification analyses of the proportion of SA-β-gal positive MRC-5 cells is shown on the right. n = 10 randomly selected microscopic fields. Scale bar, 100 μm. **e** IB analyses for indicated proteins in WCL and lysosomal fractions from MRC-5 cells at early (P18) and late (P45) passage with or without overexpressing Flag-LAMP2A-WT/3D/3A. **f** Band intensities of indicated proteins were quantified using Image J software, normalized to β-actin levels. n = 3 independent experiments. Data are presented as the means ± S.E.M. All the experiments showed consistent results in at least three independent biological replicates. Statistical significance was assessed using one-way ANOVA with Dunnett's multiple comparisons test (**d**, **f**) or two-way ANOVA with Bonferroni's multiple comparisons test (**b**). ns,

not significant. Source data are provided as a Source Data file.

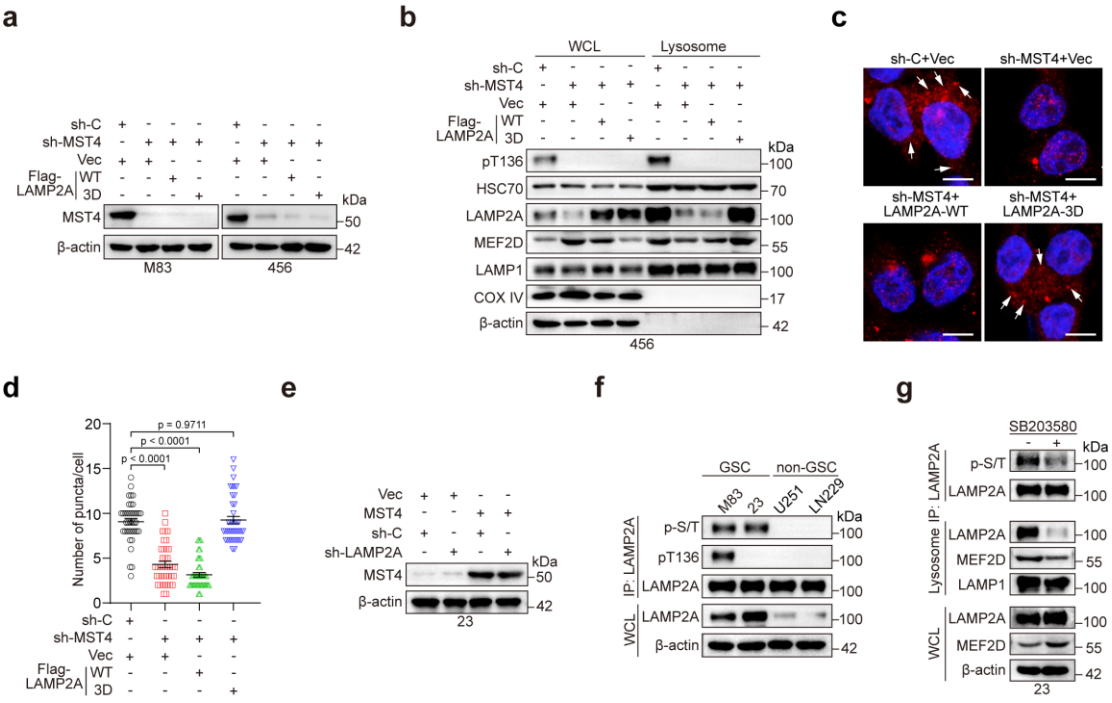

85
86
87

88 **Supplementary Figure 5: MST4-mediated phosphorylation of LAMP2A enhances CMA activity and**
89 **increases tumorigenicity in GSC cells. a** IB analyses for indicated proteins in GSC M83 and 456 cells with
90 indicated modifications. **b** IB analyses for indicated proteins in WCL and lysosomal fractions of GSC 456 cells
91 with indicated modifications. **c**, **d** Representative images (**c**) and quantification (**d**) of CMA activity detection by
92 KFERQ puncta numbers in GSC 456 cells with indicated modifications. Data are presented as the means ± S.E.M.
93 Statistical significance was assessed using one-way ANOVA with Dunnett's multiple comparisons test. n = 40
94 randomly selected cells. Scale bar, 10 μm. **e** IB analyses for indicated proteins in GSC 23 cells with indicated
95 modifications. **f** IP-IB analyses for indicated proteins in WCL of GSCs (M83 and 23) and non-GSCs (U251 and
96 LN229). **g** IP-IB analyses for indicated proteins in WCL and lysosomal fractions of GSC 23 with or without p38
97 MAPK inhibitor SB203580 (10 μM) treatment for 12 hours. All the experiments showed consistent results in at
98 least three independent biological replicates. Source data are provided as a Source Data file.

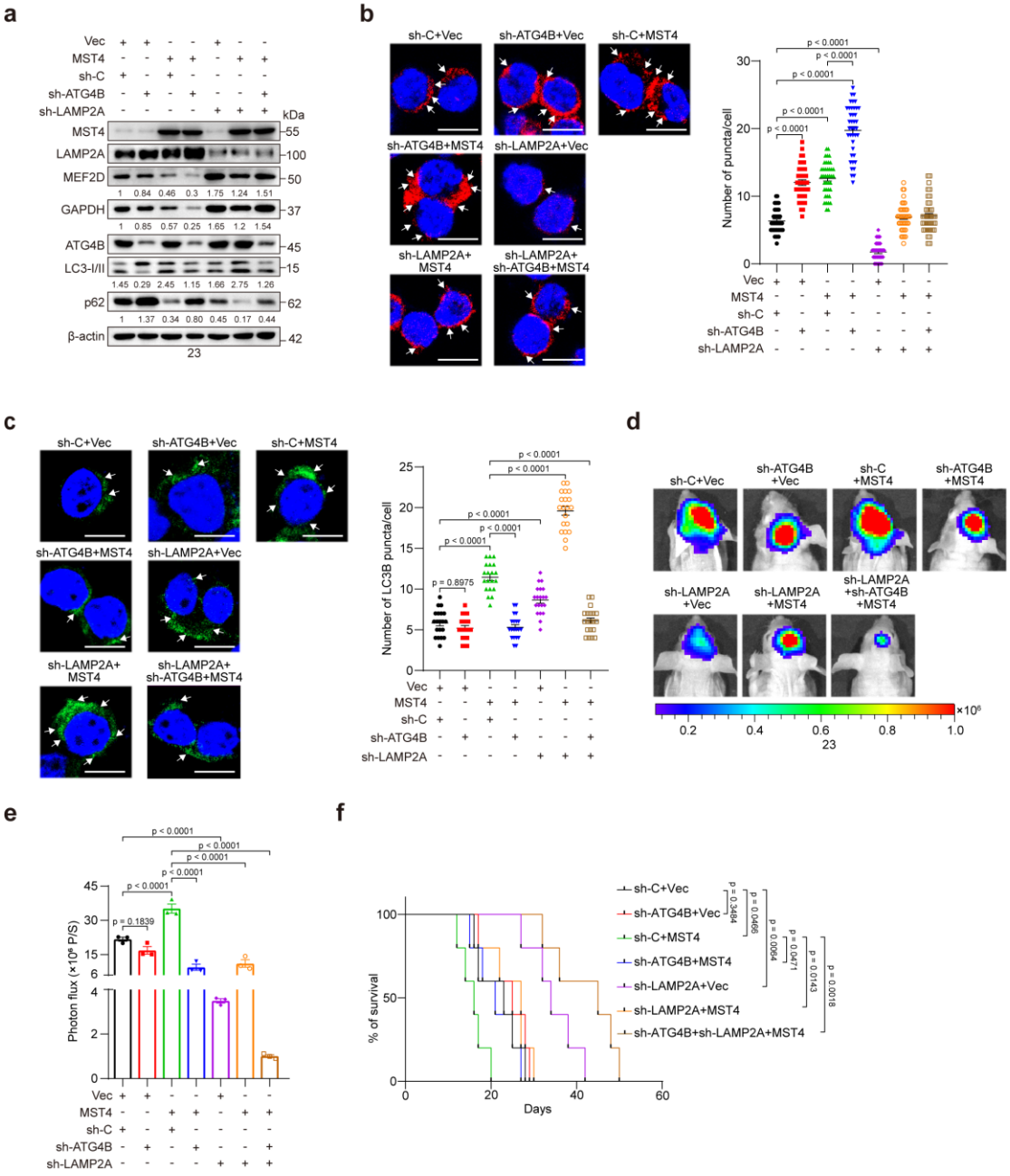
a
Vec
MST4
sh-C
sh-ATG4B
sh-LAMP2A
kDa
MST4
LAMP2A
MEF2D
GAPDH
ATG4B
LC3-I/II
p62
β-actin
55
100
50
37
45
15
62
42
23
b
sh-C+Vec
sh-ATG4B+Vec
sh-C+MST4
sh-ATG4B+MST4
sh-LAMP2A+Vec
sh-LAMP2A+ MST4
sh-LAMP2A+ sh-ATG4B+MST4
Number of puncta/cell
p < 0.0001
c
sh-C+Vec
sh-ATG4B+Vec
sh-C+MST4
sh-ATG4B+MST4
sh-LAMP2A+Vec
sh-LAMP2A+ MST4
sh-LAMP2A+ sh-ATG4B+MST4
Number of LC3B puncta/cell
p = 0.8975
d
sh-C+Vec
sh-ATG4B +Vec
sh-C +MST4
sh-ATG4B +MST4
sh-LAMP2A +Vec
sh-LAMP2A +MST4
sh-LAMP2A +sh-ATG4B +MST4
×10⁶
23
e
Photon flux (×10⁶ P/S)
p = 0.1839
f
% of survival
Days
sh-C+Vec
sh-ATG4B+Vec
sh-C+MST4
sh-ATG4B+MST4
sh-LAMP2A+Vec
sh-LAMP2A+MST4
sh-ATG4B+sh-LAMP2A+MST4
p = 0.3494
p = 0.0466
p = 0.0094
p = 0.0471
p = 0.0143
p = 0.0018

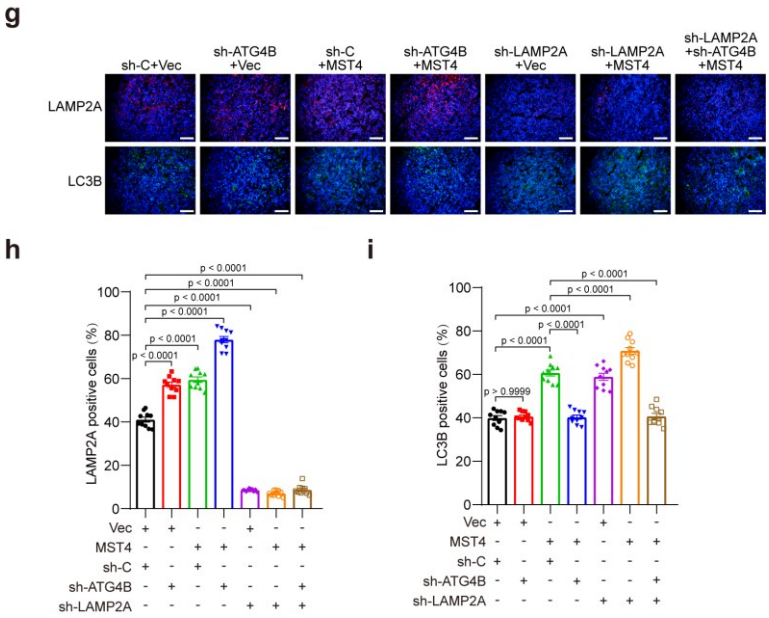

Supplementary Figure 6: MST4 mediates both activation of macroautophagy and CMA with compensatory interplay in GSCs. a IB analyses for indicated proteins in GSC 23 cells with indicated modifications. Quantifications in ratios of MEF2D, GAPDH, p62 relative to β-actin, as well as LC3B-II:-I ratios are shown. **b** Representative images (left) and quantification (right) of CMA activity detection by KFERQ puncta frequency in GSC 23 cells with indicated modifications. n = 40 randomly selected cells. Scale bar, 10 μm. **c** Representative images (left) and quantification (right) of IF staining analyses for LC3B puncta frequency in GSC 23 cells with indicated modifications. n = 20 randomly selected cells. Scale bar, 10 μm. **d** Representative luciferase-based bioluminescence images of athymic (BALB/c Nude) mice with intracranially transplanted GSC 23 cells with indicated modifications. Colored scale bars represent photons/s/cm^2/steradian. **e** Quantification of tumor bioluminescence of mice in (**d**). n = 3 mice per group. **f** Kaplan-Meier survival curves of athymic (BALB/c Nude) mice with intracranially transplanted with GSC 23 cells with indicated modifications. n = 5 mice per group. **g-i** Representative images (**g**) and quantification of IF staining for LAMP2A (**h**) and LC3B (**i**) positive cells in tumor tissues from BALB/c Nude mice intracranially transplanted with GSC 23 cells with indicated modifications. n = 10 randomly selected microscopic fields. Scale bar, 100 μm. Data are presented as the means ± S.E.M. All the experiments showed consistent results in at least three independent biological replicates. Statistical significance was assessed using one-way ANOVA with Dunnett's multiple comparisons test (**h**), one-way ANOVA with Tukey's multiple comparisons test (**b**, **c**, **e**, **i**) or log-rank test (**f**). ns, not significant. Source data are provided as a Source Data file.

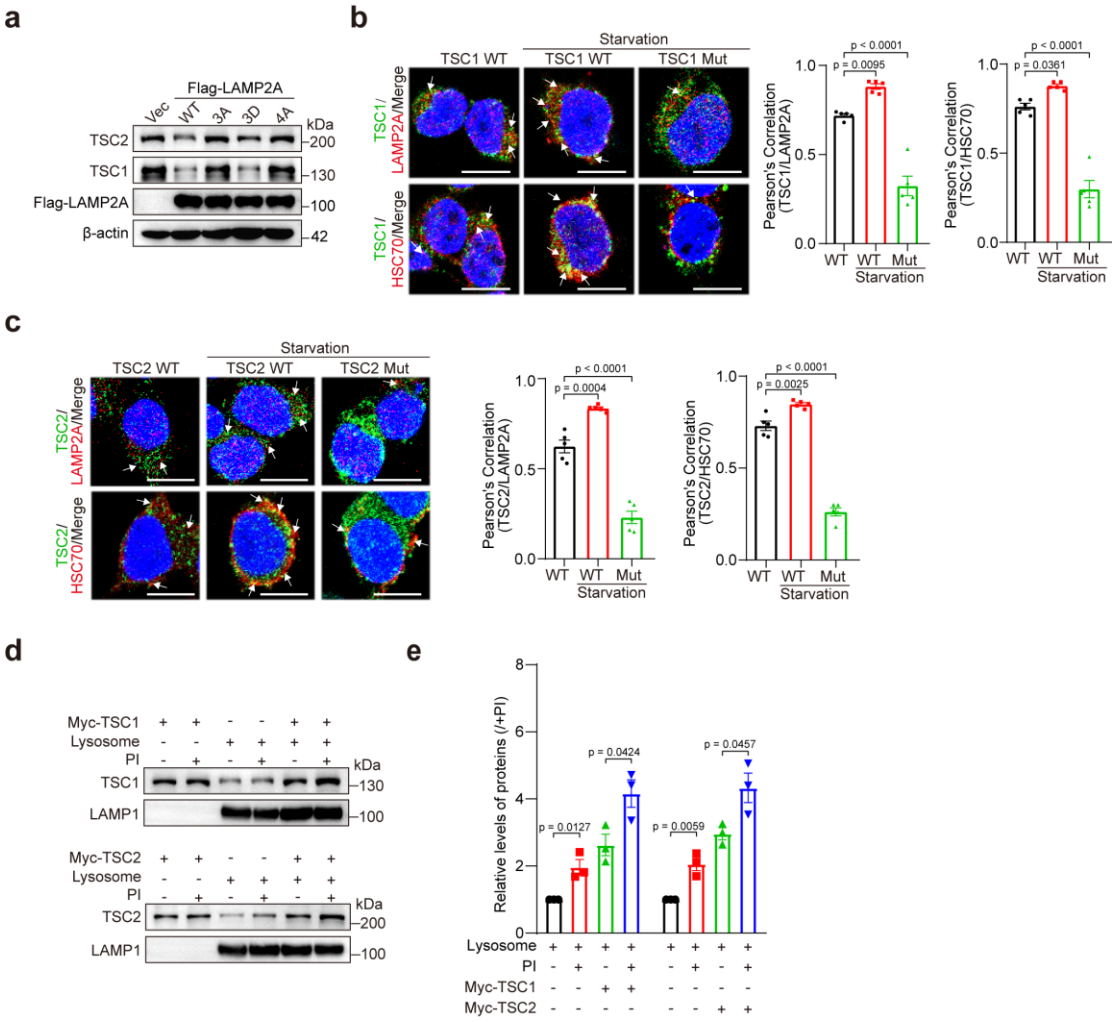

Supplementary Figure 7: TSC1/2 are identified as targets of CMA. a IB analyses for TSC1, TSC2 and Flag-LAMP2A in HEK293T cells with or without overexpressing Flag-LAMP2A-WT or mutants. **b**, **c** IF staining analyses for HEK293T cells overexpressing Myc-TSC1 (**b**) or Myc-TSC2 (**c**) using anti-LAMP2A or HSC70 and anti-Myc antibodies, with or without starvation treatment. Myc-TSC1/TSC2 (green), LAMP2A or HSC70 (red), DAPI (blue). Scale bar, 10 μm. The right panels display the quantification of Pearson's correlation between TSC1/TSC2 and LAMP2A or HSC70. n = 5 randomly selected cells. **d** In vitro lysosomal uptake assay of TSC1 (top) and TSC2 (bottom). Following co-incubation with lysosomes isolated from HEK293T cells in the presence or absence of protease inhibitor cocktail (PI), Myc-TSC1/TSC2 were internalized and degraded by lysosomes. Substrate-only reactions (without lysosomes) were included as input controls (lanes 1 and 2), while the empty lysosome samples served as the negative controls (lanes 3 and 4). LAMP1 was used to demonstrate equal lysosomal loading. **e** Quantification of TSC1 and TSC2 levels in (**d**). n = 3 independent experiments. Data are presented as the means ± S.E.M. All the experiments showed consistent results in at least three independent biological replicates. Statistical significance was assessed using one-way ANOVA with Dunnett's multiple

comparisons test (**b**, **c**), two-tailed Student's t-test (**e**). Source data are provided as a Source Data file.

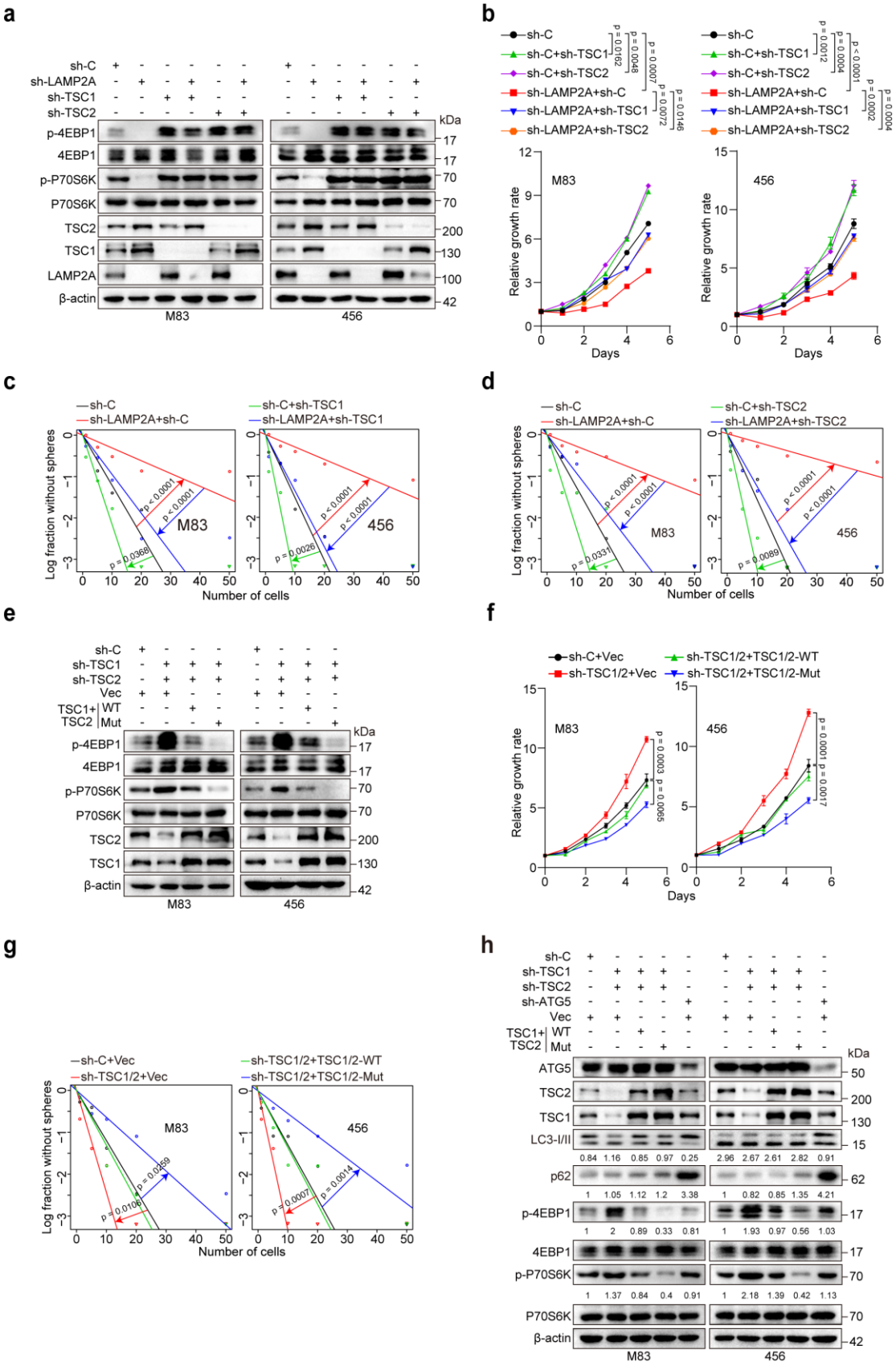
a
sh-C
sh-LAMP2A
sh-TSC1
sh-TSC2
p-4EBP1
4EBP1
p-P70S6K
P70S6K
TSC2
TSC1
LAMP2A
β-actin
kDa
M83
456
b
sh-C
sh-C+sh-TSC1
sh-C+sh-TSC2
sh-LAMP2A+sh-C
sh-LAMP2A+sh-TSC1
sh-LAMP2A+sh-TSC2
Relative growth rate
Days
c
Log fraction without spheres
Number of cells
d
e
Vec
TSC1+ TSC2 WT
Mut
f
sh-C+Vec
sh-TSC1/2+Vec
sh-TSC1/2+TSC1/2-WT
sh-TSC1/2+TSC1/2-Mut
g
h
sh-ATG5
ATG5
LC3-I/II
p62

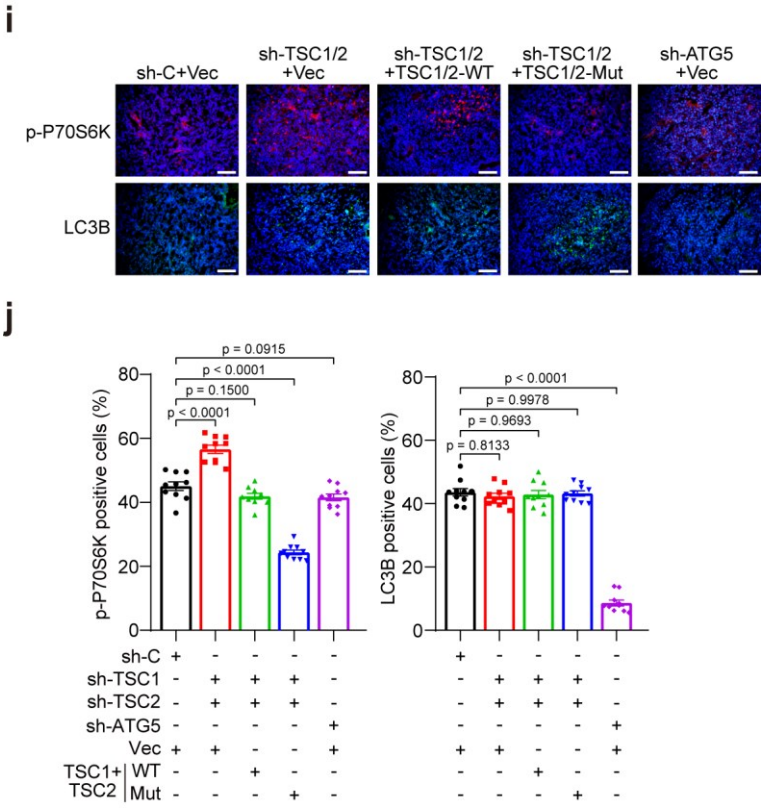

137

138 **Supplementary Figure 8: CMA enhances mTORC1 signaling and GSC self-renewal through the**
139 **degradation of TSC1/2. a** IB analyses for indicated proteins in GSC M83 and 456 cells expressing sh-C or
140 sh-LAMP2A, with or without co-expression of sh-C, sh-TSC1 or sh-TSC2. **b-d** Cell proliferation (**b**) and
141 sphere-forming frequency (**c-d**) of GSC M83 and 456 cells with indicated modifications. n = 3 independent
142 experiments. **e** IB analyses for indicated proteins in GSC M83 and 456 cells with indicated modifications. **f**, **g** Cell
143 proliferation (**f**) and sphere-forming frequency (**g**) of GSC M83 and 456 cells with indicated modifications. n = 3
144 independent experiments. **h** IB analyses for indicated proteins in GSC M83 and 456 cells with indicated
145 modifications. Quantifications in ratios of p-4EBP1, p-P70S6K, p62 relative to β-actin, as well as LC3B-II:-I ratios
146 are shown. **i**, **j** Representative images (**i**) and quantification (**j**) of IF staining for p-P70S6K and LC3B positive
147 cells in tumor tissues from BALB/c Nude mice intracranially transplanted with GSC M83 cells with indicated
148 modifications. n = 10 randomly selected microscopic fields. Scale bar, 100 μm. Data are presented as the means ±
149 S.E.M. All the experiments showed consistent results in at least three independent biological replicates. Statistical
150 significance was assessed using one-way ANOVA with Tukey's multiple comparisons test (**b**), two-sided likelihood
151 ratio tests (**c**, **d**, **g**) or one-way ANOVA with Dunnett's multiple comparisons test (**f**, **j**). ns, not significant. Source
152 data are provided as a Source Data file.

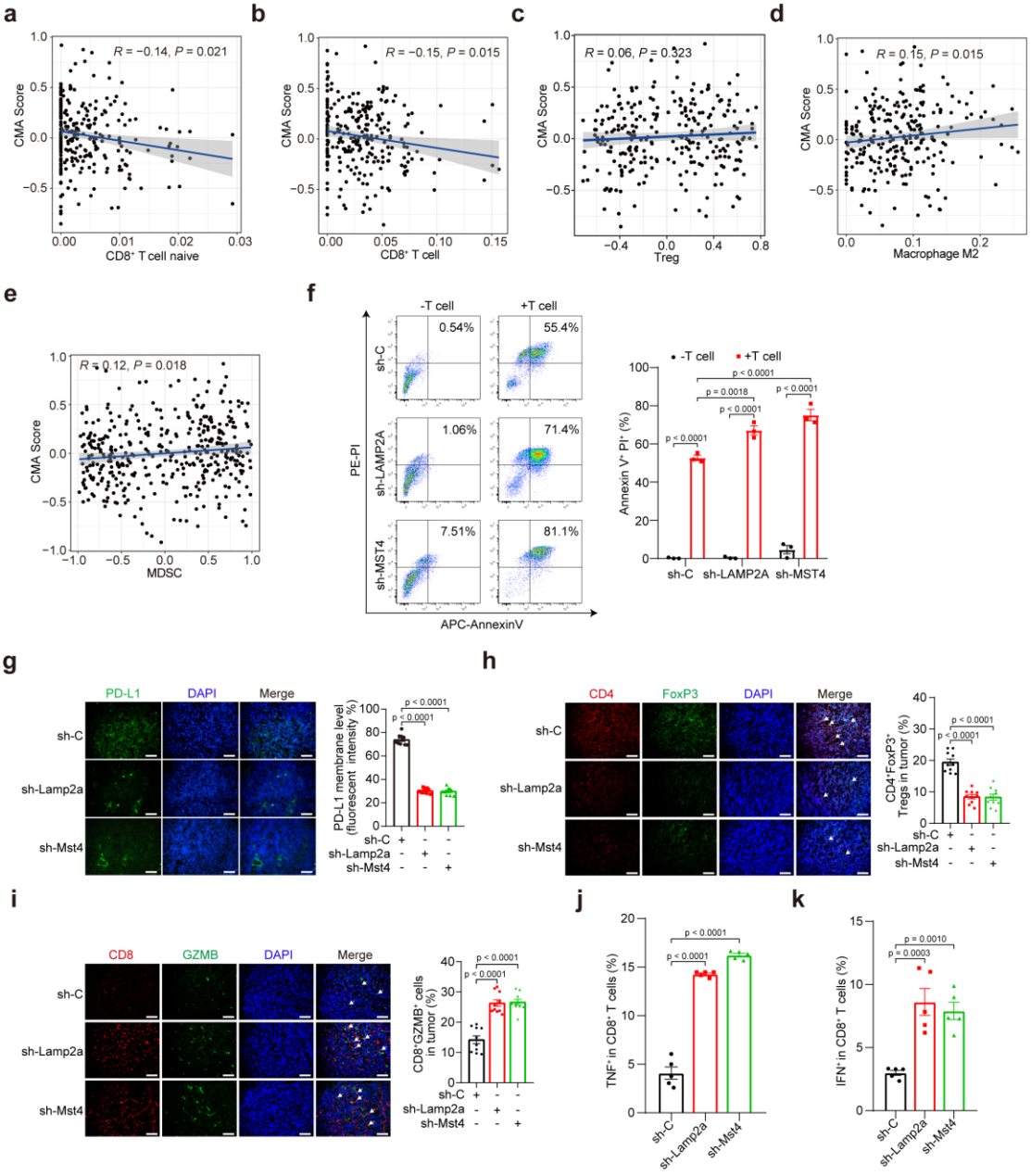
a
b
c
d
e
f
g
h
i
j
k
R = −0.14, P = 0.021
CMA Score
CD8⁺ T cell naive
R = −0.15, P = 0.015
CD8⁺ T cell
R = 0.06, P = 0.323
Treg
R = 0.15, P = 0.015
Macrophage M2
R = 0.12, P = 0.018
MDSC
-T cell
+T cell
0.54%
55.4%
1.06%
71.4%
7.51%
81.1%
sh-C
sh-LAMP2A
sh-MST4
PE-PI
APC-AnnexinV
Annexin V⁺ PI⁺ (%)
PD-L1
DAPI
Merge
sh-Lamp2a
sh-Mst4
PD-L1 membrane level (fluorescent intensity %)
CD4
FoxP3
CD4⁺FoxP3⁺ Tregs in tumor (%)
CD8
GZMB
CD8⁺GZMB⁺ cells in tumor (%)
TNF⁺ in CD8⁺ T cells (%)
IFN⁺ in CD8⁺ T cells (%)
p < 0.0001
p = 0.0018
p = 0.0010
p = 0.0003

153

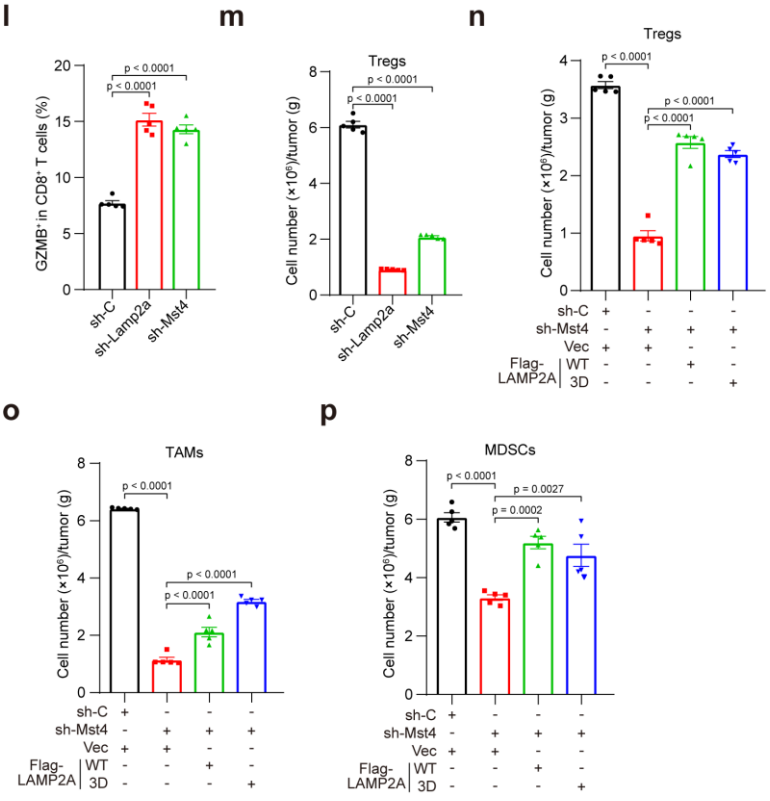

Supplementary Figure 9: CMA inhibition suppresses GBM tumorigenesis through enhanced anti-tumor immunity. a-e Correlation analysis between CMA activity scores and immune cell infiltration profiles in TCGA GBM samples using TIMER2 or TISIDB databases. **f** Apoptosis analysis of genetically modified GSC M83 cells co-cultured with or without GBM patients-derived $CD8^+$ T cells (24 h; flow cytometry). n = 3 independent experiments. PI, propidium iodide. **g** Representative images of PD-L1 immunofluorescence staining in tumor tissues from C57/BL6 mice with intracranial GL261 cells transplants with indicated modifications (left), along with quantified PD-L1 membrane levels in tumor tissue (right). n = 10 randomly selected microscopic fields. Scale bar, 100 μm. **h**, **i** Representative images (left) and quantification (right) of $CD4^+$ $FoxP3^+$ Tregs (**h**) and $CD8^+$ $GZMB^+$ cells (**i**) in tumor tissues from C57/BL6 mice with intracranial CT-2A cells transplants with indicated modifications. n = 10 randomly selected microscopic fields. Scale bar, 100 μm. **j-l** Flow cytometric analysis of population of TNF^+CD8^+ T cells (**j**), IFN^+CD8^+ T cells (**k**) and $GZMB^+CD8^+$ T cells (**l**) in infiltrating $CD8^+$ T cells from tumor tissues of C57/BL6 mice with intracranial CT-2A cells transplants with indicated modifications. n = 5 independent experiments. **m-p** Flow cytometric analyses for population of infiltrating Tregs (**m**, **n**), TAMs (**o**) and MDSCs (**p**) in tumor tissues from C57/BL6 mice with intracranial CT-2A cells transplants with indicated modifications. n = 5 independent experiments. Data are presented as the means ± S.E.M. All the experiments showed consistent results in at least three independent biological replicates. Statistical significance was assessed

using one-way ANOVA with Tukey's multiple comparisons test (**f**, **n**-**p**) or one-way ANOVA with Dunnett's multiple comparisons test (**g**-**m**). Source data are provided as a Source Data file.

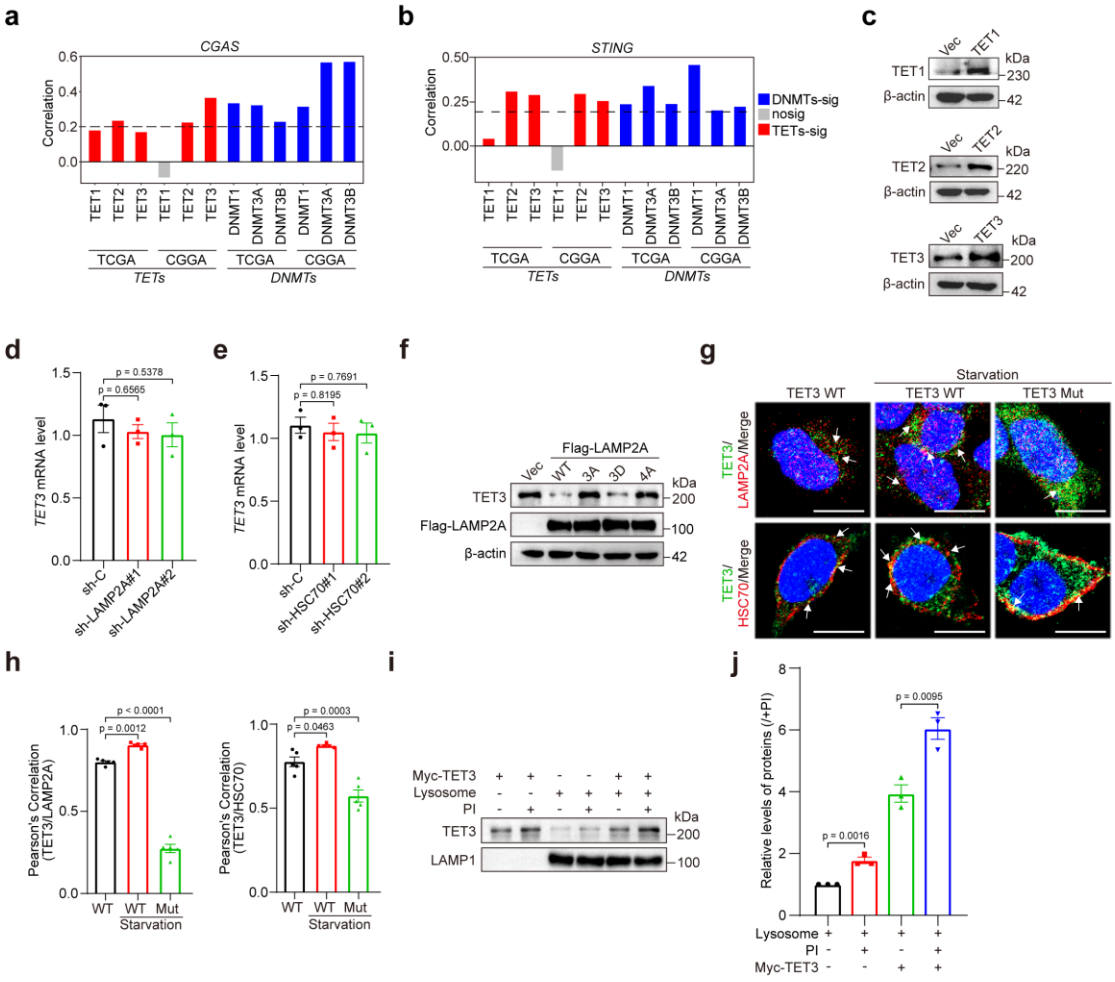

Supplementary Figure 10: TET3 undergoes lysosomal degradation through CMA. a, **b** Correlation assessments of *CGAS* (**a**) and *STING* (**b**) expression levels in relation to *TETs* and DNA methyltransferases (*DNMTs*) utilizing TCGA and CGGA datasets. **c** IB analyses for TET1, TET2 or TET3 in HEK293T cells transfected with either the Vector control or expressing TET1, TET2 and TET3, respectively. **d**, **e** qPCR assessment of mRNA level of *TET3* in HEK293T cells with or without LAMP2A (**d**) or HSC70 (**e**) knock down. n = 3 independent experiments. **f** IB analyses for indicated proteins in HEK293T cells with or without overexpressing Flag-LAMP2A-WT or mutants. **g** IF staining analyses for HEK293T cells overexpressing Myc-TET3 using anti-Myc and anti-LAMP2A or HSC70 antibodies. Myc-TET3 (green), LAMP2A or HSC70 (red), DAPI (blue). Scale bar, 10 μm. **h** Quantification of Pearson's correlation between TET3 and LAMP2A or HSC70. n = 5 randomly selected cells. **i** In vitro lysosomal uptake assay of TET3. Following co-incubation with lysosomes isolated from HEK293T cells in the presence or absence of protease inhibitor cocktail (PI), Myc-TET3 were internalized and degraded by lysosomes. Substrate-only reactions (without lysosomes) were included as input controls (lanes 1 and 2), while the empty lysosome samples served as the negative controls (lanes 3 and 4).

LAMP1 was used to demonstrate equal lysosomal loading. **j** Quantitative analysis of TET3 protein levels from panel **i**. n = 3 independent experiments. Data are presented as the means ± S.E.M. All the experiments showed consistent results in at least three independent biological replicates. Statistical significance was assessed using one-way ANOVA with Dunnett's multiple comparisons test (**d**, **e**, **h**) or two-tailed Student's t-test (**j**). ns, not significant. Source data are provided as a Source Data file.

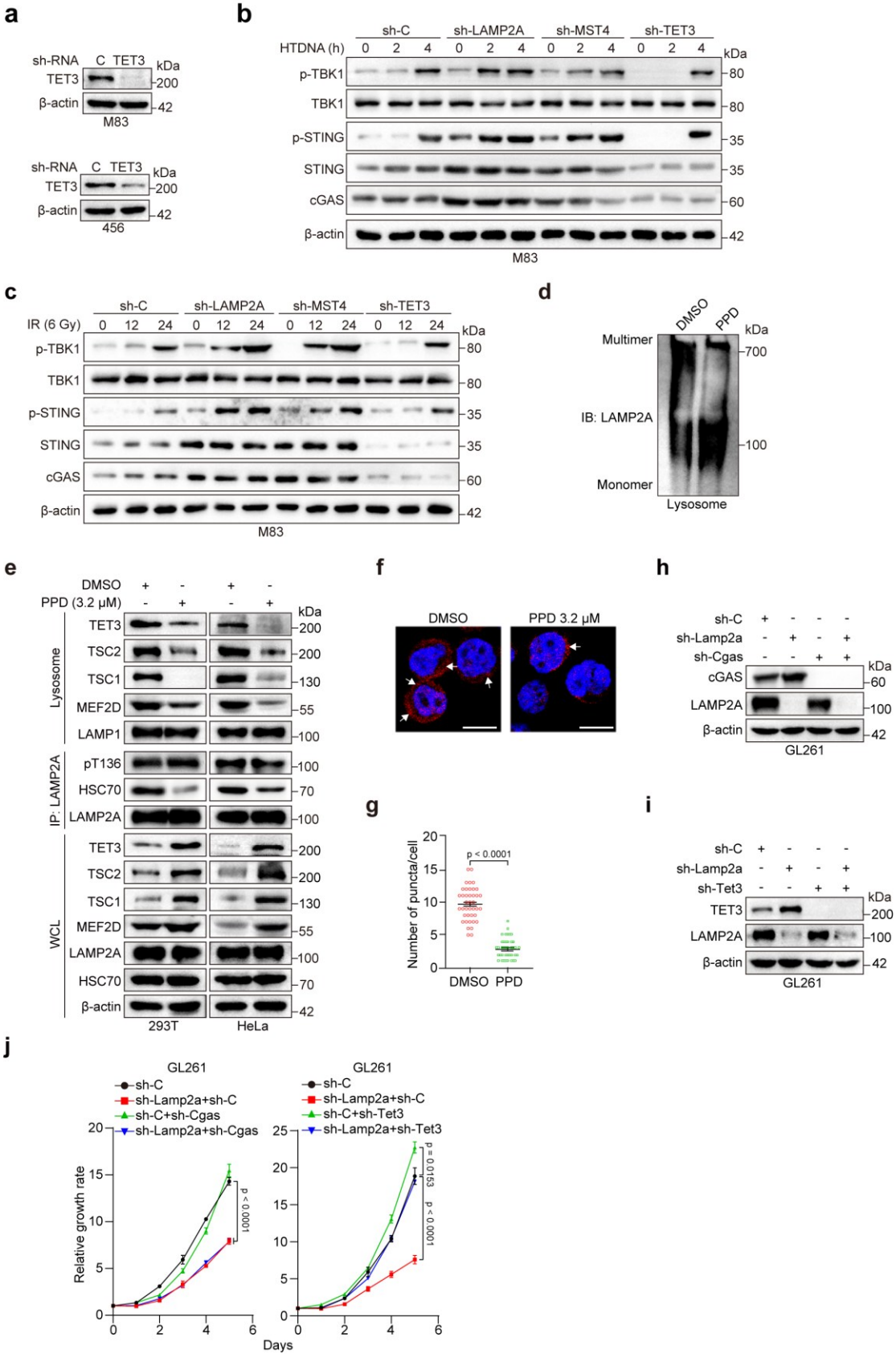

Supplementary Figure 11: CMA modulates cGAS/STING signaling through regulation of TET3. a IB analyses for TET3 in GSC M83 and 456 cells expressing sh-C or sh-TET3. **b**, **c** IB analyses for indicated proteins

in GSC M83 cells treated with 1 μg/mL HT-DNA for indicated time (**b**) or after subjected to 6 Gy IR stimulation for indicated time (**c**). **d** Purified lysosomes from HEK293T cells, with or without 3.2 μM PPD treatment, were analyzed using native continuous gel electrophoresis and subjected to IB detection of LAMP2A. **e** IP-IB analyses for indicated proteins in WCL, as well as IB analyses for indicated proteins in lysosomal fractions of HEK293T and HeLa cells with or without 3.2 μM PPD treatment. **f**, **g** Representative images (**f**) and quantification (**g**) of KFERQ puncta in GSC M83 cells with or without 3.2 μM PPD treatment. n = 40 randomly selected cells. Scale bar, 10 μm. **h**, **i** IB analyses for cGAS (**h**) or TET3 (**i**) and LAMP2A in GL261 cells with indicated modifications. **j** Cell proliferation of GL261 cells with indicated modifications. n = 3 independent experiments. Data are presented as the means ± S.E.M. All the experiments showed consistent results in at least three independent biological replicates. Statistical significance was assessed using two-tailed Student's t-test (**g**) or one-way ANOVA with Dunnett's multiple comparisons test (**j**). Source data are provided as a Source Data file.

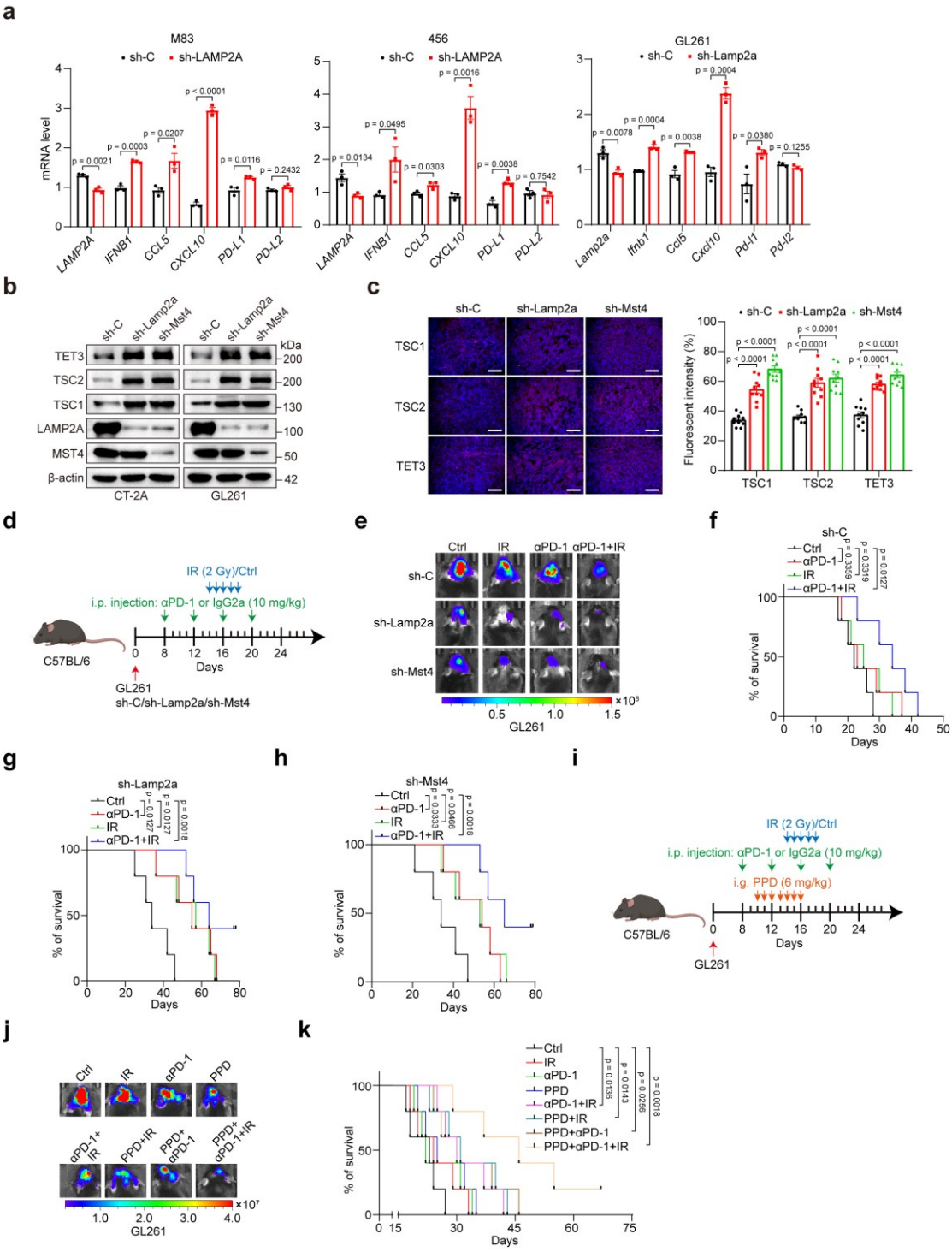
a
M83
456
GL261
sh-C
sh-LAMP2A
sh-Lamp2a
mRNA level
LAMP2A
IFNB1
CCL5
CXCL10
PD-L1
PD-L2
Lamp2a
Ifnb1
Ccl5
Cxcl10
Pd-l1
Pd-l2
b
sh-C
sh-Lamp2a
sh-Mst4
kDa
TET3
TSC2
TSC1
LAMP2A
MST4
β-actin
CT-2A
GL261
c
sh-C
sh-Lamp2a
sh-Mst4
TSC1
TSC2
TET3
Fluorescent intensity (%)
d
IR (2 Gy)/Ctrl
i.p. injection: αPD-1 or IgG2a (10 mg/kg)
C57BL/6
Days
GL261
sh-C/sh-Lamp2a/sh-Mst4
e
Ctrl
IR
αPD-1
αPD-1+IR
sh-C
sh-Lamp2a
sh-Mst4
GL261
f
sh-C
Ctrl
αPD-1
IR
αPD-1+IR
% of survival
Days
g
sh-Lamp2a
h
sh-Mst4
i
IR (2 Gy)/Ctrl
i.p. injection: αPD-1 or IgG2a (10 mg/kg)
i.g. PPD (6 mg/kg)
C57BL/6
GL261
j
Ctrl
IR
αPD-1
PPD
αPD-1+ IR
PPD+IR
PPD+ αPD-1
PPD+ αPD-1+IR
GL261
k
Ctrl
IR
αPD-1
PPD
αPD-1+IR
PPD+IR
PPD+αPD-1
PPD+αPD-1+IR
% of survival
Days

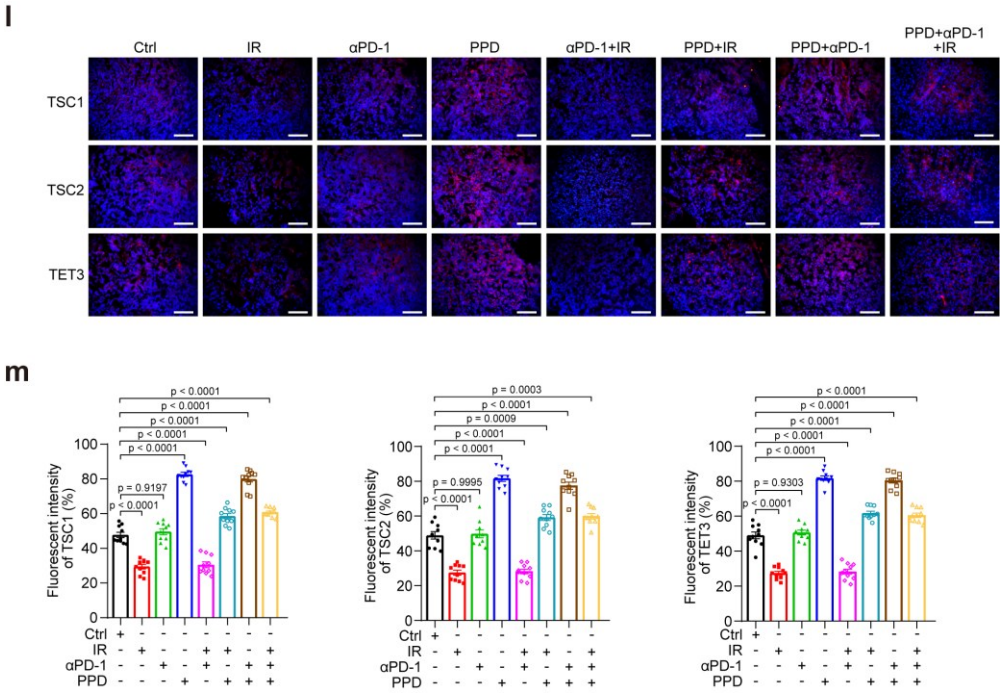

Supplementary Figure 12: Inhibition of CMA activity improved the effectiveness of radiation and anti-PD-1 treatments against tumors. a mRNA levels of *LAMP2A*, *IFNB1*, *CCL5*, *CXCL10*, *PD-L1* and *PD-L2* were detected in GSC M83, GSC 456 and GL261 cells. n = 3 independent experiments. **b** IB analyses for indicated proteins in CT-2A and GL261 cells expressing sh-C, sh-Lamp2a or sh-Mst4. **c** Representative IF staining images (left) and quantification (right) for fluorescent intensity of TSC1, TSC2 and TET3 in tumor tissues from C57BL/6 mice with intracranial CT-2A cells transplants with indicated modifications. n = 10 randomly selected microscopic fields. Scale bar, 100 μm. **d**, **i** Scheme representing the experimental procedure, created with BioRender.com. **e** Representative luciferase-based bioluminescence images of C57BL/6 mice with intracranially transplanted GL261 cells with indicated modifications and treatments. Colored scale bars represent photons/s/cm^2/steradian. **f-h** Kaplan-Meier survival curves of C57BL/6 mice with intracranially transplanted with GL261 cells with modifications and treatments. n = 5 mice per group. **j** Representative luciferase-based bioluminescence images of C57BL/6 mice with intracranially transplanted GL261 cells with indicated treatments. Colored scale bars represent photons/s/cm^2/steradian. **k** Kaplan-Meier survival curves of C57BL/6 mice with intracranially transplanted with GL261 cells with indicated treatments. n = 5 mice per group. **l**, **m** Representative IF staining images (**l**) and quantification (**m**) for fluorescent intensity of TSC1, TSC2 and TET3 in tumor tissues from C57BL/6 mice with intracranial CT-2A cells transplants with indicated modifications. n = 10 randomly selected microscopic fields. Scale bar, 100 μm. Data are presented as the means ± S.E.M. All the experiments showed consistent results in at least three

227 independent biological replicates. Statistical significance was assessed using two-tailed Student's t-test (**a**),
228 one-way ANOVA with Dunnett's multiple comparisons test (**c**, **m**) or log-rank test (**f**, **g**, **h**, **k**). ns, not significant.
229 Source data are provided as a Source Data file.
230

Supplementary Table 1: KFERQ-like motifs in following proteins.

Protein names	Canonical KFERQ motif	position	mutation
TSC1	DRLIQ	[650:654]	DALIQ
TSC1	DVKLQ	[932:936]	DVALQ
TSC2	RKELQ	[350:354]	AAELQ
TSC2	ERLLQ	[366:370]	EALLQ
TET3	ELIRQ	[574:578]	ELIAQ
TET3	QIKIE	[621:625]	QIAIE
TET3	QIVEK	[698:702]	QIVEA
TET3	QKEKL	[1042:1046]	QAEAL
TET3	EKIKQ	[1050:1054]	EAIAQ

Supplementary Table 2: sh-RNA target sequences.

Target	sequence
homo-sh-LAMP2A	1# 5′-TCTAGTGTTGCTGGCTTATTT-3′
	2# 5′-AATCTGCAACCTGATTGATTA-3′
homo-sh-MST4	1# 5′-AAGGATAGGTGTTTGGTAATG-3
	2# 5′-CCTCTTGGTGTATAGTATTTA-3′
homo-sh-HSC70	1# 5′-GCAACTGTTGAAGATGAGAAA-3′
	2# 5′-ACATTTGAAGGACCTAAATTC-3′
homo-sh-TSC1	1# 5′-AAAGAAGAAGCTGCAATATCT-3′
	2# 5′-GTGCAATATGAGGCCAAATTT-3′
homo-sh-TSC2	1# 5′-GAGGGTAAACAGACGGAGTTT-3′
	2# 5′-CTGGAGAGGTAATAACTTA-3′
homo-sh-TET1	1# 5′-GCAGCTAATGAAGGTCCAGAA-3′
	2# 5′-CCTTGATAGAATCACTCAGTT-3
homo-sh-TET2	1# 5′-GTAGAGGGTATTCCAAGTG-3′
	2# 5′-CAAGAACAGGAAGTATAGT-3′
homo-sh-TET3	1# 5′-GAAAGATGAAGGTCCATATTA-3′
	2# 5′-GGTCGTATAATGGCATATTAA-3′
mus-sh-Lamp2a	5′-TGGAACTTTCATTCGGAAATT-3′
mus-sh-Mst4	5′-AGATTTAGAGGAAGCTATTAA-3′
mus-sh-Cgas	5′-CCTCTTTAGGATTGTCAGAAT-3′
mus-sh-Tet3	5′-CGCCCACAAGGACCAACATAA-3′
homo-sh-ATG4B	1#5'-CAGCGTCCTCAACGCATTCAT-3′
	2#5'-GTGGTTGGTTTGGAATTAAAG-3′
homo-sh-ATG5	1#5'-CCTTTCATTCAGAAGCTGTTT-3′
	2#5'-CCTGAACAGAATCATCCTTAA-3′

Supplementary Table 3: Primers for plasmid construction.

Target	Sequence
pCDH-HA-MST4	F: 5'-GACTATGCAGGATCCATGGCCCACTCGCCGGT-3'
	R: 5'-ATCCTTCGCGGCCGCTTAGGGGGATTCGTCTGCTGAAC-3'
pCDH-Flag-MST4	F: 5'-ACCGAGCTCGGATCCATGGCCCACTCGCCGGT-3'
	R: 5'-ATCCTTCGCGGCCGCTTAGGGGGATTCGTCTGCTGAAC-3'
pCDH-Flag-LAMP2A	F: 5'-ACCGAGCTCGGATCCATGGTGTGCTTCCGCCTC-3'
	R: 5'-ATCCTTCGCGGCCGCCTAAAATTGCTCATATCCAGCATGATGGTG-3'
pCMV6-Myc-TSC1	F: 5'-GCCATGGAGGCCCGAATTCAAATGGCCCAACAAGCAAATGTC-3'
	R: 5'-GATCCCCGCGGCCGCTTAGCTGTGTTCATGATGAGTCTCATTG-3'
pCMV6-Myc-TSC2	F: 5'-GCCATGGAGGCCCGAATTCAAATGGCCAAACCAACAAGCAAA-3'
	R: 5'-GATCCCCGCGGCCGCTCACACAAACTCGGTGAAGTCCTC-3'
pCMV6-Myc-TET1	F: 5'-GCCATGGAGGCCCGAATTCAAATGTCTCGATCCCGCCATG-3'
	R: 5'-GATCCCCGCGGCCGCTCAGACCCAATGGTTATAGGGCCC-3'
pCMV6-Myc-TET2	F: 5'-GCCATGGAGGCCCGAATTCAAATGGAACAGGATAGAACCAACC-3'
	R: 5'-GATCCCCGCGGCCGCTCATATATATCTGTTGTAAGGCCCTGTGAC-3'
pCMV6-Myc-TET3	F: 5'-GCCATGGAGGCCCGAATTCAAATGAGCCAGTTTCAGGTGC-3'
	R: 5'-GATCCCCGCGGCCGCCTAGATCCAGCGGCTGTAGGG-3'
pET-28a-His-LAMP2A	F: 5'-ATGGGTCGCGGATCCATGGTGTGCTTCCGCCTC-3'
	R: 5'-GTGGTGGTGCTCGAGCTAAAATTGCTCATATCCAGCATGATGGTG-3'

Supplementary Table 4: Primers for qRT-PCR.

Target	Sequence
homo *ACTB*	F: 5'-AGCGAGCATCCCCCAAAGTT-3'
	R: 5'-GGGCACGAAGGCTCATCATT-3'
homo *LAMP2A*	F: 5'-TATGTGCAACAAAGAGCAGA-3'
	R: 5'-CAGCATGATGGTGCTTGAGA-3'
homo *IFNB1*	F: 5'-GCTTGGATTCCTACAAAGAAGCA-3'
	R: 5'-ATAGATGGTCAATGCGGCGTC-3'
homo *CGAS*	F: 5'-TAACCCTGGCTTTGGAATCAAAA-3'
	R: 5'-TGGGTACAAGGTAAAATGGCTTT-3'
homo *STING*	F: 5'-CCAGAGCACACTCTCCGGTA-3'
	R: 5'-CGCATTTGGGAGGGAGTAGTA-3'
homo *TET3*	F: 5'-TCCAGCAACTCCTAGAACTGAG-3'
	R: 5'-AGGCCGCTTGAATACTGACTG-3'
homo *CCL5*	F: 5'-CCAGCAGTCGTCTTTGTCAC-3'
	R: 5'-CTCTGGGTTGGCACACACTT-3'
homo *CXCL10*	F: 5'-GTGGCATTCAAGGAGTACCTC-3'
	R: 5'-TGATGGCCTTCGATTCTGGATT-3'
homo *PD-L1*	F: 5'-GGACAAGCAGTGACCATCAAG-3'
	R: 5'-CCCAGAATTACCAAGTGAGTCCT-3'
homo *PD-L2*	F: 5'-ATTGCAGCTTCACCAGATAGC-3'
	R: 5'-AAAGTTGCATTCCAGGGTCAC-3'
mus *Actb*	F: 5'-GTGACGTTGACATCCGTAAAGA-3'
	R: 5'-GCCGGACTCATCGTACTCC-3'
mus *Lamp2a*	F: 5'-TGTATTTGGCTAATGGCTCAGC-3'
	R: 5'-TATGGGCACAAGGAAGTTGTC-3'
mus *Ifnb1*	F: 5'-AGCTCCAAGAAAGGACGAACA-3'
	R: 5'-GCCCTGTAGGTGAGGTTGAT-3'
mus *Ccl5*	F: 5'-GCTGCTTTGCCTACCTCTCC-3'
	R: 5'-TCGAGTGACAAACACGACTGC-3'
mus *Cxcl10*	F: 5'-CCAAGTGCTGCCGTCATTTTC-3'
	R: 5'-GGCTCGCAGGGATGATTTCAA-3'
mus *PD-L1*	F: 5'-GCTCCAAAGGACTTGTACGTG-3'
	R: 5'-TGATCTGAAGGGCAGCATTTC-3'
mus *PD-L2*	F: 5'-CTGCCGATACTGAACCTGAGC-3'
	R: 5'-GCGGTCAAAATCGCACTCC-3'